

Cite this article as: Li Li, Zhao Wei, Feng Zhixue, et al. Interfacial Microstructure and Shear Strength of $Ti_{50}Al_{50}$ Joint Vacuum Brazed with Ti-Cu-Ni-Nb-Al-Zr-Hf Amorphous Filler Alloy[J]. Rare Metal Materials and Engineering, 2022, 51(02): 378-385.

ARTICLE

Interfacial Microstructure and Shear Strength of $Ti_{50}Al_{50}$ Joint Vacuum Brazed with Ti-Cu-Ni-Nb-Al-Zr-Hf Amorphous Filler Alloy

Li Li^{1,2}, Zhao Wei¹, Feng Zhixue¹, Zhang Yuxin¹, Huang Zhichao¹, Li Xiaoqiang²

¹ School of Materials Science & Engineering, East China Jiaotong University, Nanchang 330013, China; ² National Engineering Research Center of Near-Net-Shape Forming for Metallic Materials, South China University of Technology, Guangzhou 510640, China

Abstract: Amorphous Ti-9.5Cu-8Ni-8Nb-7Al-2.5Zr-1.8Hf (wt%) filler alloy was employed to vacuum braze $Ti_{50}Al_{50}$ (at%) alloy at the brazing temperatures ranging from 1140 to 1220 °C for 30 min. The effect of brazing temperature on the microstructure and shear strength of the brazed joints was investigated. Results show that all the brazed joints are mainly divided into three reaction layers regardless of the brazing temperature, and both of α_2 - Ti_3Al and $Ti_2Cu(Ni)$ phases exist in each reaction layer, but their size and distribution change significantly with brazing temperature, especially the $Ti_2Cu(Ni)$ phase in isothermal solidification layer II. The continuous α_2 - Ti_3Al layer I is stable below 1200 °C but breaks and loses its barrier effect above 1200 °C. It is notable that the α_2 - Ti_3Al precipitated in the brazed seam can act as a nucleation inhibitor and refine the crystal grain. Shear test results show that the average shear strength of $Ti_{50}Al_{50}$ brazed joints first increases and then decreases with brazing temperature and the maximum shear strength of 184 MPa is obtained at 1180 °C. α_2 - Ti_3Al mainly occupies the fracture surface with cleavage characteristics.

Key words: $Ti_{50}Al_{50}$ (at%) alloy; Ti-Cu-Ni-Nb-Al-Zr-Hf amorphous filler; vacuum brazing; microstructure; shear strength

TiAl-based alloys are important engineering materials, which possess desirable properties such as low density, good specific strength and creep resistance as well as good corrosion resistance and high-temperature mechanical properties, and thus they are widely used in aerospace and automotive industries^[1-3]. Nonetheless, they also have some restrictive defects such as poor wear resistance, poor machinability and intrinsic brittleness^[4]. In order to give full play to the advantages of TiAl alloys, it is necessary to achieve reliable connection of TiAl alloys. Compared with diffusion bonding^[5,6], friction welding^[7] and TIG/MIG welding^[8], brazing is considered as an effective connection method due to its low operating temperature, convenience and cost-effectiveness as well as high-quality joint and low residual stress, which is widely used to join TiAl alloys. Song^[9] and Cai et al^[10] also reported that the brazing can be

employed reliably to join TiAl-based alloys to themselves.

It is vital to select suitable filler alloy to join TiAl alloy so as to obtain better brazed joint. According to the previous study^[10], Al-based and Ag-based filler alloys have been employed to join TiAl-based alloy, while the joint have the problems of weak high-temperature strength, low service temperature and poor corrosion resistance^[11,12]. Ti-based filler has intrinsic affinity with TiAl alloy, and in addition, Ti-based filler alloy possesses good joining performance and creep resistance due to the better wettability between Ti-based filler and TiAl substrate^[13,14]. Therefore, we selected Ti-based filler to braze TiAl-based alloy in vacuum atmosphere. At present, the research on Ti-based filler mainly concentrates on the pure Ti filler, Ti-Cu-Ni, Ti-Zr-Cu-Ni and Ti-Ni-Nb system filler metals. Li et al^[15] investigated reactive brazing of γ -TiAl alloy and GH99 with pure Ti foil as filler metal, but the liquidus

Received date: February 07, 2021

Foundation item: National Natural Science Foundation of China (51865012); Natural Science Foundation of Jiangxi Province (20202BABL204040); Open Foundation of National Engineering Research Center of Near-Net-Shape Forming for Metallic Materials, China (2016005); Science Foundation of Educational Department of Jiangxi Province, China (GJJ170372); GF Basic Research Project, China (JCKY2016603C003); Research Project of Special Furnishment and Part, China (JPPT125GH038)

Corresponding author: Li Xiaoqiang, Ph. D., Professor, National Engineering Research Center of Near-Net-Shape Forming for Metallic Materials, Guangzhou 510640, P. R. China, Tel: 0086-20-87111080, E-mail: lixq@scut.edu.cn

Copyright © 2022, Northwest Institute for Nonferrous Metal Research. Published by Science Press. All rights reserved.

temperature of the pure Ti foil is very high (about 1660 °C) so a higher brazing temperature is required, which will affect the microstructure of TiAl substrate. The commercially common Ti-15Cu-15Ni and Ti-15Cu-25Ni filler alloys can successfully braze TiAl alloys, but it is easy to form overmuch Ti-Cu system (such as Ti₂Cu) or Ti-Ni system (such as TiNi₃) intermetallics in the brazed seam, which are harmful to the joint strength [16]. According to Ti-Zr, Ti-Cu and Ti-Ni binary alloy phase diagrams [17], Zr is completely miscible with Ti and the liquidus temperature decreases with increasing the Zr when the content of Zr is less than 40at%, so increasing the Zr content and decreasing the content of Cu and Ni can reduce the formation of brittle Ti-Cu/Ni system intermetallic compounds. Al element can improve the affinity and wettability of filler alloy with the TiAl substrate and have a solid solution strengthening effect on the filler alloy. Nb is an active and high melting point structural element, which can be completely miscible with Ti. Nb addition can increase the high-temperature heat resistance and chaos of Ti-based filler alloy. The chemical property of Hf is similar to that of Ti and Hf addition can improve the amorphous forming ability of Ti-based filler alloy. Meanwhile, Zr, Hf and Ti belong to the group IVB element and have similar lattice type and chemical property, so the addition of Zr and Hf can form continuous solid solution in Ti alloy and improve the supercooled liquid stability of Ti-based filler alloy as well as increase mixing enthalpy of filler alloy and further promote the amorphous forming ability of Ti-based filler alloy [18-20]. According to Ref. [19] and Ti-Al binary alloy phase diagram [17], Al is an important α -stabilizer and the addition of Al element can improve the $\alpha \leftrightarrow \beta$ transition temperature of titanium alloy. When the content of Al ranges from 35at% to 48at%, Ti-Al alloys form a two-phase equilibrium between α_2 -Ti₃Al and γ , and the eutectoid reaction of $\gamma + \alpha_2 \leftrightarrow \alpha$ occurs at 1125 °C. With increasing the Al content to 50at%, the phase transition temperature of Ti₅₀Al₅₀ alloys with single γ phase is up to about 1350 °C, and thus the higher brazing temperature can be allowed to use. In order to give full play to the superior high-temperature advantage of Ti₅₀Al₅₀ alloys, we designed a novel filler of Ti-Cu-Ni-Nb-Al-Zr-Hf alloy containing relatively lower Cu and Ni contents and a quantitative amount of Al and Nb as well as a bit of Zr and Hf element. According to the previous studies [21,22], amorphous alloys, owing to their

advantages of uniform element distribution, good spreadability and adhesiveness with respect to the crystalline filler, have been developed to braze TiAl alloy.

In the present work, the Ti₅₀Al₅₀ (at%) alloy was vacuum brazed with amorphous filler Ti-9.5Cu-8Ni-8Nb-7Al-2.5Zr-1.8Hf (wt%), and the influence of brazing temperature on the microstructure and shear strength of the joints as well as the formation mechanism of interfacial microstructure were investigated.

1 Experiment

The experimental base material was Ti₅₀Al₅₀ (at%) alloy and the brazed sample was cut into 8 mm×6 mm×3 mm by wire cut electro discharge machine. The chemical composition of the amorphous filler was Ti-9.5Cu-8Ni-8Nb-7Al-2.5Zr-1.8Hf (wt%), and the preparation methods are as follows. First, under high purity argon atmosphere, the filler alloy ingot was prepared by arc-melting in a water-cooled copper mold six times and then homogenized at 900 °C for 4 h to reduce segregation. Second, after induction melting in a quartz tube, rapid solidification was implemented by the single-roller melt spinning technique with a rotating Cu wheel at a circumferential speed of 30 m/s. The resulting filler foil had a ribbon shape with 10~11 mm in width and about 80 μ m in thickness, and the eventual size of the filler foil for brazing was about 10 mm×8 mm×60 μ m. The stand-by surfaces of all samples were finally ground by 800# sandpaper and ultrasonically cleaned in acetone for 10 min before brazing. The schematic diagrams of the metallographic and shear test samples are shown in Fig. 1a and 1b, respectively.

The assembled specimens were brazed in HP-12×12×12 vacuum furnace with a vacuum degree of $\sim 1.33 \times 10^{-2}$ Pa, the brazing temperature ranged from 1140 °C to 1220 °C and the holding time was 30 min. After brazing, the samples were cooled to room temperature with the furnace cooling. And then the cross-sections of brazed joint were ground to 3000# grit, polished and etched. Shear test was carried out at a constant speed of 0.5 mm/min by a universal testing machine (AG-X100KN, the schematic diagram is shown in Fig. 1c). Scanning electron microscopy (SEM) with energy dispersive spectrometer (EDS) was used to examine the joint interfacial microstructure, elemental distribution and fracture surface after shear test. Transmission electron microscopy (TEM) and

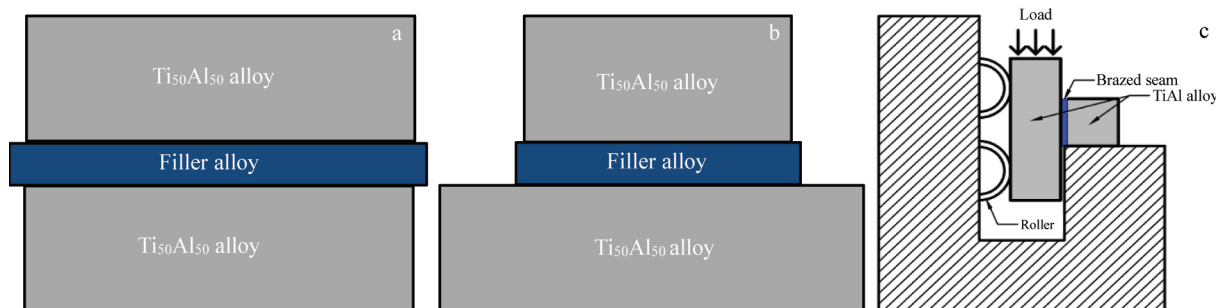


Fig.1 Schematic diagrams of metallographic sample (a), shear test sample (b) and shear test setup (c)

X-ray diffractometer (XRD) were employed to identify the phase composition of the brazed seam and the fracture surface after shear testing, respectively. The melting behavior of the amorphous Ti-Cu-Ni-Nb-Al-Zr-Hf filler was investigated by differential scanning calorimetry (DSC) at a heating rate of 20 °C/min, and the result showed that its melting temperature is 1131 °C.

2 Results and Discussion

2.1 Interfacial microstructure of the typical $Ti_{50}Al_{50}$ brazed joint

Fig. 2 presents the interfacial microstructure of the TiAl joint brazed at 1180 °C for 30 min. No cracks or pores can be observed in the brazed seam and the phases of brazed joint are uniformly distributed, indicating that a good metallurgical bonding occurs between the amorphous filler foil and $Ti_{50}Al_{50}$ substrate. According to the different microstructural morphologies of the brazing seam, the brazed joint can be divided into three reaction layers, marked as I, II and III in

Fig.2a. Combining the content of Zr and Hf in the amorphous filler with the element line scanning across the brazed joint along the bold white line (marked in Fig.2a), it can be seen that the Ni/Cu, Zr and Hf are mainly distributed in layer II and the diffused depth of Ni/Cu into the TiAl substrate is significantly more than that of Zr and Hf, which may be due to the better affinity of Ni/Cu with TiAl alloy and much more concentration gradient compared with Zr/Hf as well as the relatively low diffusion rate during brazing due to the larger atomic radii of Zr and Hf. The high magnification backscattered electron images (BEIs) of each layer are shown in Fig.2c~2e. It is observed that the morphologies of layers I and III mainly consist of light gray phases marked as spot A and E and continuous lamellar phases marked as zone B and D in Fig. 2c and 2e. Layer II is mainly composed of continuous gray blocky phase marked as zone C in Fig. 2d. The corresponding EDS results of each spot are listed in Table 1. The α_2 - Ti_3Al phase exists in each layer of the brazed seam, which can be attributed to the continuous dissolution of Al

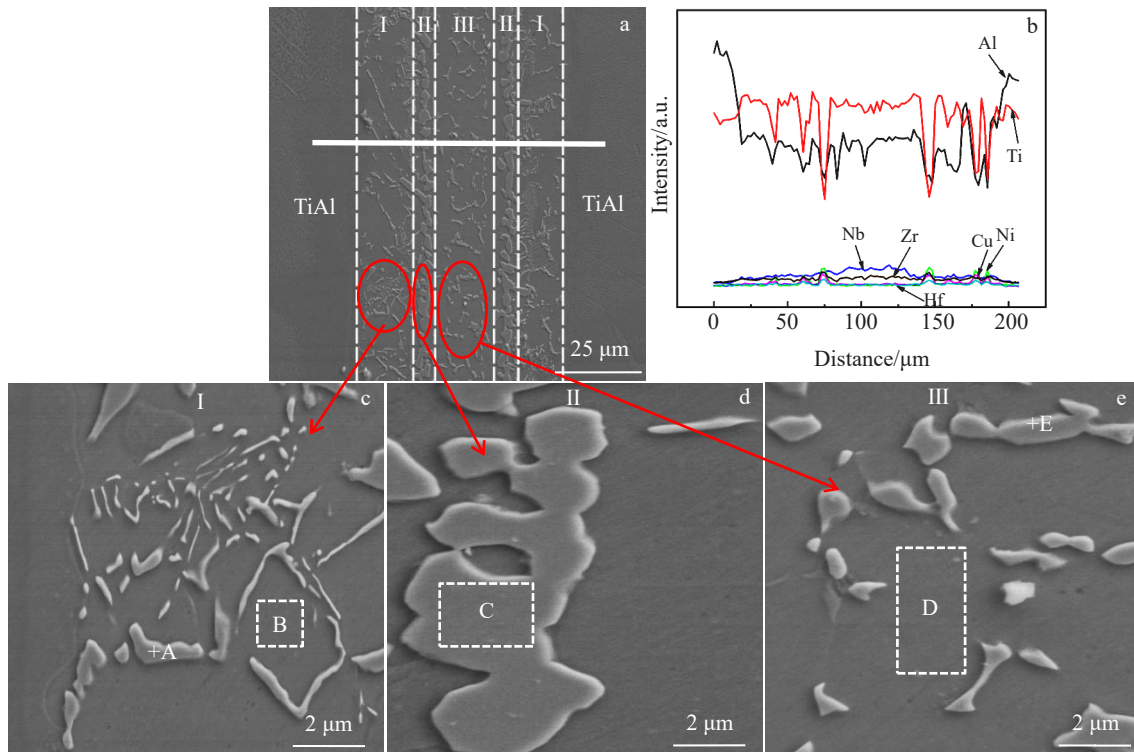


Fig.2 Backscattered electron images (BEIs) of the $Ti_{50}Al_{50}$ joint brazed at 1180 °C for 30 min: (a) integral interfacial microstructure, (b) EDS line scanning results (b), and (c~e) high magnification BEIs of layers I, II and III

Table 1 EDS results of each spot/zone in Fig.2c~2e

Spot/Zone	Element content/at%							Possible phase
	Ti	Al	Cu	Ni	Nb	Zr	Hf	
A	51.55	11.48	14.69	15.37	3.85	2.29	0.77	$Ti_2Cu(Ni)+\alpha_2-Ti_3Al$
B	60.98	32.57	2.29	1.83	1.85	0.28	0.20	α_2-Ti_3Al
C	45.15	16.02	18.09	15.97	2.85	1.29	0.63	$Ti_2Cu(Ni)$
D	64.61	31.80	1.08	0.28	1.97	0.18	0.08	α_2-Ti_3Al
E	57.59	11.14	16.3	13.36	0.67	0.66	0.28	$Ti_2Cu(Ni)+\alpha_2-Ti_3Al$

atom from TiAl substrate into the molten filler and the diffusion of filler alloy into TiAl substrate in brazed process. From the beginning of heating to the melting of the filler alloy, the Al atoms from the dissolution of TiAl substrate diffuse into brazed seam and react with Ti element to form α_2 -Ti₃Al phase. According to Ti-Al binary alloy phase diagram^[17], eutectoid reaction of α -Ti $\leftrightarrow\alpha_2$ -Ti₃Al+ γ -TiAl occurs at 1125 °C and the maximum temperature of transformation from single α_2 -Ti₃Al into α -Ti is 1180 °C. Once the continuous α_2 -Ti₃Al phase layer (such as layer I) is formed, it will become a barrier to prevent the diffusion of Ni and Cu atoms from the molten filler into the TiAl substrate, and the Ni and Cu atoms will be enriched in layer II because their outward diffusion needs a larger driving force. In fact, the layer II is easy to reach the limit solid solution due to the enrichment of Ni and Cu, resulting in restrained diffusion of Cu and Ni away from the molten filler alloy. The remnant liquid forms the layer III during the subsequent cooling stage. According to the micromorphology, we can find that a small amount of light gray phases (marked as spot A and E) are distributed in layers I and III, but exist in layer II as a continuous blocky phase (marked as C). The EDS analysis results indicate that A and E are Ti₂Cu(Ni) with α_2 -Ti₃Al, B and D mainly are α_2 -Ti₃Al, and C is mainly Ti₂Cu(Ni).

The TEM was used to further identify these phases in each layer, and the corresponding TEM images and selected area electron diffraction (SAED) patterns are shown in Fig.3. The microstructural morphologies in Fig.3a~3c show that the layer I mainly consists of the gray phase (marked as A) and dark phase (marked as B). Combining the SAED patterns in Fig.3d, 3e and the corresponding EDS results (listed in Table 2), it can be confirmed that A and B are Ti₃Al phases. The phase of point C (marked in Fig.3b) is determined as Ti₂Cu(Ni) by the

EDS analysis and the corresponding SAED pattern, which is consistent with the analysis result of layer II in Fig. 2. Similarly, gray blocky phase (marked as D in Fig.3c) also can be verified as α_2 -Ti₃Al.

2.2 Microstructure evolution mechanism of Ti₅₀Al₅₀ brazed joint

Based on the previous analysis in Section 2.1, a theoretic microstructure evolution model for TiAl/Ti-Cu-Ni-Nb-Al-Zr-Hf/TiAl joint is established, as shown in Fig.4. Generally, the formation of the interfacial microstructure of the brazed joint originates from the diffusion reaction of elements, so the whole reaction process can be divided into two stages.

Stage one: when the temperature is lower than the glass transition temperature (T_g) of the amorphous filler, just only physical contact, atomic-solid interdiffusion, slight deformation and chemical metallurgical reaction occur between the TiAl substrate and the amorphous filler, as shown in Fig.4a. When the temperature is increased to the solidus temperature (T_s) of the filler, the amorphous filler gradually transforms from solid state to unstable supercooled liquid state, which usually accelerates the element interdiffusion of TiAl substrate and filler, then crystallizes and finally begins to melt. Further increasing the temperature to the liquidus temperature (T_l), the filler completely melts into liquid state and the diffusion rate of Al atom from the dissolved TiAl substrate into the molten filler zone as well as that of Ni and Cu atoms in the liquid filler alloy toward TiAl parent alloy are accelerated, as shown in Fig.4b. Generally, the diffusion rate of atoms in the liquid state is much faster than in the solid state.

Stage two: as shown in Fig.4c, with increasing the diffusion depth and the reaction degree between TiAl substrate and liquid filler within holding time, the interfacial reaction layers gradually form in the brazed joint, namely, solid-state

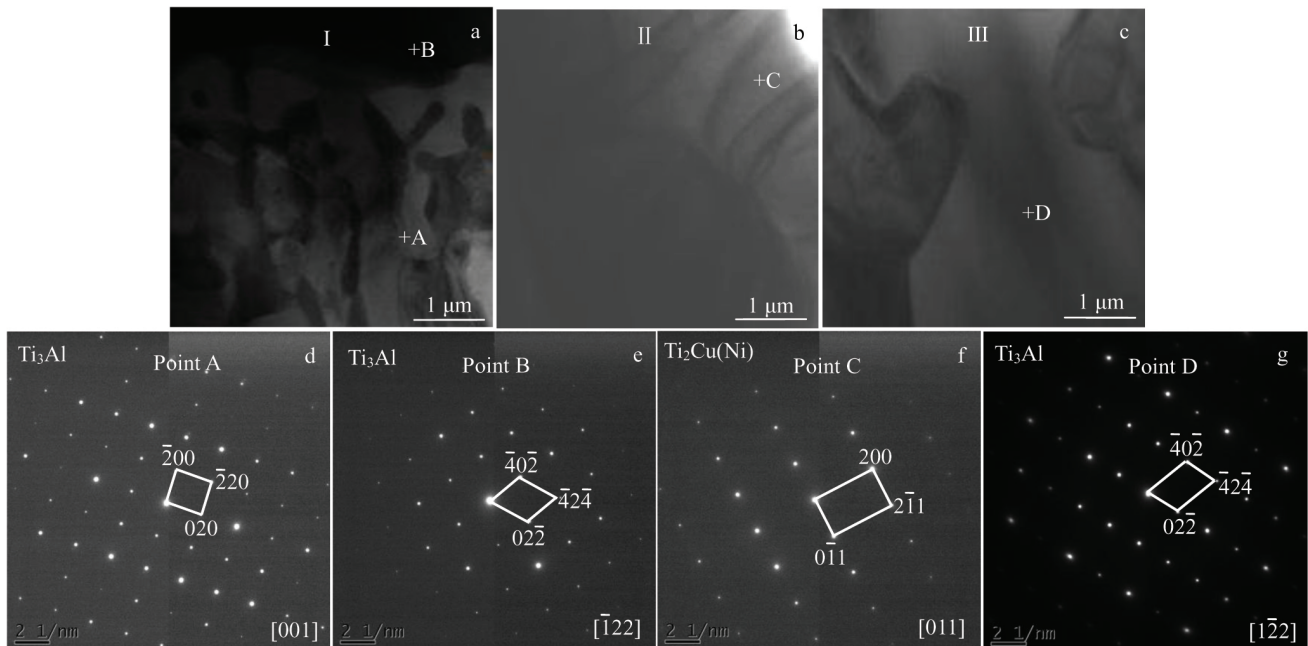


Fig.3 TEM images (a~c) and corresponding SAED patterns (d~g) of points in layers I, II and III in Fig.3a~3c

Table 2 EDS results of points in Fig.3a~3c

Point	Element content/at%						
	Ti	Al	Cu	Ni	Nb	Zr	Hf
A	65.65	29.27	2.09	1.33	1.15	0.38	0.13
B	67.86	25.34	2.60	1.80	1.82	0.35	0.23
C	47.78	19.93	14.52	13.97	1.42	1.95	0.43
D	63.73	30.78	1.58	1.32	0.91	0.95	0.73

diffusion layer, isothermal solidification layer and residual molten filler layer. The diffusion of Al atoms from TiAl substrate plays an important role in the formation and the microstructure evolution of brazed joint. The Al atom from the dissolution of TiAl parent alloy will diffuse toward the filler alloy zone and react with Ti to form α_2 -Ti₃Al when its content ranges from 22at% to 47at%^[17]. Generally, the inward diffusion of filler alloy atoms into the parent alloy can give rise to the change of the micromorphology^[20]. And the diffused atoms are insufficient to decrease the T_s of TiAl substrate to below the brazing temperature, which will facilitate the formation of solid-state diffusion layer. According to the previous analysis result of Fig.2, this layer is mainly composed of α_2 -Ti₃Al phase with Ti₂Cu(Ni) phase. Once the continuous α_2 -Ti₃Al layer is formed, it will restrict the atomic interdiffusion between filler alloy and TiAl substrate. The liquidus temperature of the molten filler alloy next to TiAl substrate is increased up to above the brazing temperature by the dissolution of TiAl parent alloy, leading to formation of the isothermal solidification layer in the soaking time. Meanwhile, the Cu and Ni atoms in the molten filler will

continuously diffuse toward the isothermal solidification layer, resulting in the enrichment of Cu and Ni and formation of Ti₂Cu(Ni) in this layer. The residual liquid filler zone mainly contains a certain amount of Ti, Al and Cu/Ni atoms which react with each other to form α_2 -Ti₃Al and Ti₂Cu(Ni) phases, as shown in Fig. 4d, and then precipitate in the subsequent cooling process, leading to the formation of residual filler layer.

2.3 Effect of brazing temperature on microstructure of Ti₅₀Al₅₀ brazed joints

Fig. 5 shows the BEIs of Ti₅₀Al₅₀ joints brazed at different brazing temperatures for 30 min. All the brazed joints are mainly divided into three reaction layers regardless of the brazing temperature. The interfacial morphology of the TiAl brazed joint was observed at different brazing temperatures within 1140~1220 °C for 30 min, the phase constitution in each reaction layer hardly changes with increasing the brazing temperature, but the size and distribution of each phase change significantly, especially in layer II. It may be related to the atomic diffusion coefficient at different temperatures, which can be calculated by the Arrhenius equation ($D = D_0 \exp(-Q/k_B T)$)^[23]. Obviously, the atomic diffusion coefficient increases with increasing the temperature. Significant change in micromorphology of layer II with the temperature indicates that intensive interactions and metallurgical reaction occur.

When the brazing temperature is 1140 °C, the existed and scattered evenly continuous α_2 -Ti₃Al layer I restricts the diffusion of Cu and Ni atoms into TiAl substrate, resulting in enrichment of Cu and Ni in isothermal solidification layer II.

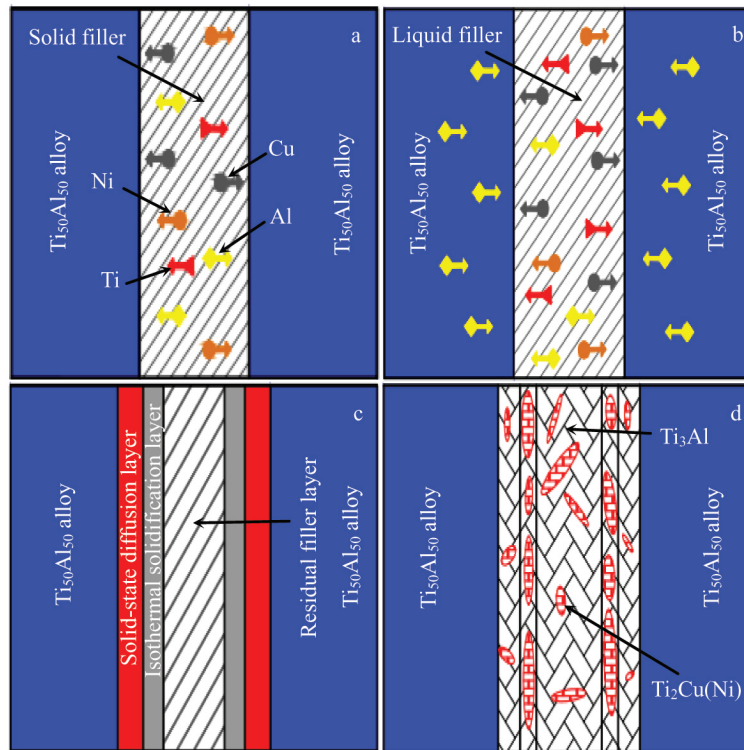


Fig.4 Formation mechanism model of Ti₅₀Al₅₀ joint brazed with Ti-based amorphous filler: (a, b) stage one and (c, d) stage two

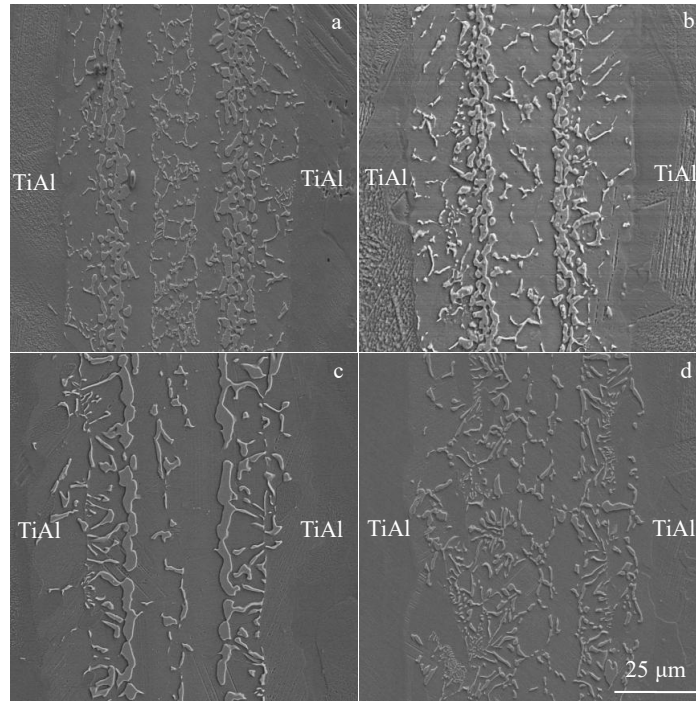


Fig.5 BEIs of $Ti_{50}Al_{50}$ joints brazed at different temperatures for 30 min: (a) 1140 °C, (b) 1160 °C, (c) 1200 °C, and (d) 1220 °C

With increasing of the brazing temperature from 1160 °C to 1180 °C, the atomic diffusion rate is accelerated, the content of Al atom gradually increases in the central brazed layer, and more filler alloy atoms (especially Cu and Ni) mainly diffuse to the side of TiAl parent alloy and enrich in layer II, (as shown in Fig. 5b and Fig. 2a). Therefore, more continuous blocky $Ti_2Cu(Ni)$ phase forms in the layer II and the content of $Ti_2Cu(Ni)$ phase decreases in layer III. But the interfacial morphology of layer I has almost no changes, which may be attributed to the barrier effect of the stable α_2-Ti_3Al layer under 1200 °C. Once the brazing temperature exceeds 1200 °C, the barrier equilibrium of α_2-Ti_3Al layer is broken and the atomic interdiffusion between TiAl substrate and the molten filler alloy increases sharply, the Cu and Ni atoms further diffuse into layer I. When the brazing temperature is

increased to 1220 °C, the size of each phase in different reaction layers becomes refined as shown in Fig.5d. It may be related to the higher content of α_2-Ti_3Al with the high melting point preferentially precipitated in the seam brazed at 1220 °C contrast to the case at 1200 °C, which acts as a nucleation inhibitor and promotes the grain nucleation rate faster than the growth rate, resulting in the refinement of crystal grain. Accordingly, this further verifies the importance of the brazing temperature on the size and distribution of the interfacial microstructure in brazed joint.

2.4 Evaluation of shear strength and fracture morphology of $Ti_{50}Al_{50}$ brazed joint

The variation of shear strength of the joints brazed at different brazing temperatures for 30 min is shown in Fig.6a. The shear strength increases firstly when the brazing

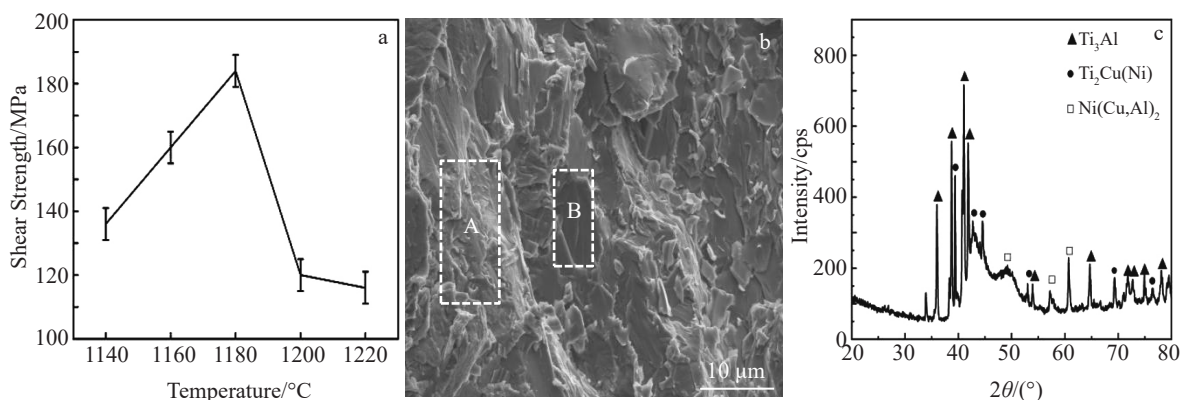


Fig.6 Shear strength of $Ti_{50}Al_{50}$ joints brazed at different temperatures (a), fracture morphology of the joint brazed at 1180 °C for 30 min (b), and XRD pattern of fracture surface (c)

Table 3 EDS results of zones marked in Fig.6b

Zone	Element content/at%						
	Ti	Al	Cu	Ni	Nb	Zr	Hf
A	56.45	31.51	5.95	3.66	2.17	0.14	0.12
B	62.50	33.78	0.51	0.20	2.63	0.25	0.13

temperature ranges from 1140 °C to 1180 °C and then decreases with further increasing the brazing temperature. The maximum shear strength of 184 MPa is obtained at 1180 °C. When the brazing temperature is lower (such as 1140 °C), due to the insufficient atomic diffusion and metallurgical reaction between the TiAl parent alloy and Ti-Cu-Ni-Nb-Al-Zr-Hf amorphous filler alloy, the shear strength of the brazed joint is only 136 MPa. Increasing the brazing temperature can accelerate more sufficient interdiffusion and metallurgical reaction, which is beneficial to obtain sound bonding. Therefore, the shear strength of the joint brazed at 1160 °C is increased to 160 MPa. And the inflection point of joint strength occurs at 1180 °C, which is related to the remarkable change of the interfacial morphology resulted from transformation of single α_2 -Ti₃Al to α -Ti at 1180 °C. Once the brazing temperature exceeds 1200 °C, the α_2 -Ti₃Al \rightarrow α -Ti or β -Ti congruent transformation occurs and the continuous α_2 -Ti₃Al layer I loses the barrier effect, which sharply increases the atomic diffusion between TiAl parent alloy and the molten filler alloy. Furthermore, the residual stress in the brazed joint increases with the temperature and high residual stress can weaken the joint strength, so the shear strength of the TiAl joint brazed at 1200 °C is significantly decreased to 120 and 116 MPa at 1220 °C. Compared with the case at the brazing temperature of 1200 °C, much more Al atoms diffuse into brazed seam and form the high melting point α_2 -Ti₃Al at brazing temperature of 1220 °C. The α_2 -Ti₃Al precipitated in the brazed seam can act as a nucleation inhibitor and refine the crystal grain, which can offset the effect of residual stress on the joint strength. Therefore, the shear strength of the TiAl joint brazed at 1220 °C only slightly decreases compared with at 1200 °C. The fracture morphology of the Ti₅₀Al₅₀ brazed joint is presented in Fig.6b, and the fracture surface presents a step-like distribution and a typical cleavage fracture characteristics. The EDS results (listed in Table 3) show that the phases (marked as A and B in zones Fig. 6b) of fracture surface are mainly α_2 -Ti₃Al, which is further determined by the XRD analysis of the fracture surface (Fig. 6c). Accordingly, the α_2 -Ti₃Al should be controlled in the brazing seam so as to obtain robust joint.

3 Conclusions

1) Sound Ti₅₀Al₅₀ (at%) brazed joints can be obtained using the amorphous Ti-9.5Cu-8Ni-8Nb-7Al-2.5Zr-1.8Hf (wt%) as filler alloy and the brazed joint consists mainly of three reaction layers: solid-state diffusion layer I, isothermal solidification layer II and the residual filler layer III. The phase compositions are mainly α_2 -Ti₃Al and Ti₂Cu(Ni) in the brazed joints at different brazing temperatures.

2) Brazing temperature exerts an important effect on the interfacial morphology of the Ti₅₀Al₅₀ brazed joints due to the atomic diffusion coefficient at different temperatures. At brazing temperatures lower than 1200 °C, the continuous α_2 -Ti₃Al layer I is stable which restricts the diffusion of Cu and Ni atoms into TiAl substrate, leading to enrichment of Cu and Ni in layer II and formation of blocky Ti₂Cu(Ni). Once the brazing temperature exceeds 1200 °C and up to 1220 °C, the barrier equilibrium of α_2 -Ti₃Al layer is broken and the atomic interdiffusion between TiAl substrate and molten filler alloy increases sharply, so Cu and Ni decrease in content but Al content increases in the center filler layer III, and the content of α_2 -Ti₃Al also increases in the brazing seam. Meanwhile, the α_2 -Ti₃Al with a high melting point preferentially precipitated in the brazed seam can act as a nucleation inhibitor and refine the crystal grain.

3) The shear strength of Ti₅₀Al₅₀ brazed joints increases firstly and then decreases with brazing temperature in the range of 1140~1220 °C for 30 min. The maximum shear strength is about 184 MPa at 1180 °C. The fracture surface of the TiAl brazed joint exhibits typical brittle cleavage characteristics and the α_2 -Ti₃Al phase occupies most of the fracture surface.

References

- 1 Qi Xiansheng, Xue Xiangyi, Tang Bin et al. *Rare Metal Materials and Engineering*[J], 2015, 44(7): 1575
- 2 Wang Xiufeng, Ma Mo, Liu Xuebin et al. *Transactions of Nonferrous Metals Society of China*[J], 2006, 16(5): 1059
- 3 Wang Y, Cai X Q, Yang Z W et al. *Journal of Materials Science & Technology*[J], 2017, 33: 682
- 4 Zhang S Z, Zhao Y B, Zhang C J et al. *Materials Science and Engineering A*[J], 2017, 200: 366
- 5 Zhu Lei, Li Jingshan, Tang Bin et al. *Vacuum*[J], 2019, 164: 140
- 6 Ren H S, Xiong H P, Chen B et al. *Materials Science and Engineering A*[J], 2016, 651: 45
- 7 Chen X, Xie F Q, Ma T J et al. *Journal of Alloys and Compounds* [J], 2015, 646: 490
- 8 Miao Yugang, Ma Zhaowei, Yang Xiaoshan et al. *Journal of Materials Processing Technology*[J], 2018, 260: 104
- 9 Song Xiaoguo, Si Xiaoqing, Cao Jian et al. *Rare Metal Materials and Engineering*[J], 2018, 47(1): 52
- 10 Cai Y S, Liu R C, Zhu Z W et al. *Intermetallics*[J], 2017, 91: 35
- 11 Li Li, Zhao Wei, Feng Zhixue et al. *Transactions of Nonferrous Metals Society of China*[J], 2020, 30(8): 2143
- 12 Xu Zhiwu, Li Zhengwei, Chai Ben et al. *Journal of Alloys and Compounds*[J], 2020, 815: 152 493
- 13 Li Li, Li Xiaoqiang, Hu Ke et al. *Materials Science and Engineering A*[J], 2015, 634: 91
- 14 Shiue R K, Wu S K, Chen Y T et al. *Intermetallics*[J], 2008, 16(9): 1083
- 15 Li Haixin, He Peng, Lin Tiesong et al. *Transactions of Nonferrous Metals Society of China*[J], 2012, 22: 324

- 16 Shiue R K, Wu S K, Chen Y T. *Intermetallics*[J], 2010, 18(1): 107
- 17 Massalaki T B. *Binary Alloy Phase Diagrams*[M]. ASM International: Materials Park,1990
- 18 Zhang Qiang, Sun Liangbo, Liu Qingyong et al. *Journal of the European Ceramic Society*[J], 2017, 37(3): 931
- 19 Leyens Christoph, Peters Manfred. *Titanium and Titanium Alloys* [M]. New York: Wiley-VCH, 2003
- 20 Sekulić Dušan-p. *Advances in Brazing-Science, Technology and Applications*[M]. Philadelphia: Woodhead Publishing Limited, 2013
- 21 Liu Y H, Hu J D, Shen P et al. *Materials & Design*[J], 2013, 47: 281
- 22 Liu Yuhua, Hu Jiandong, Zhang Yaping et al. *Journal of Materials Science & Technology*[J], 2011, 27(7): 653
- 23 Ren H S, Ren X Y, Xiong H P et al. *Materials & Characterization*[J], 2019, 155: 109 813

Ti-Cu-Ni-Nb-Al-Zr-Hf非晶钎料合金真空钎焊 Ti₅₀Al₅₀接头的界面组织与剪切强度

李 力^{1,2}, 赵 巍¹, 冯志雪¹, 张玉鑫¹, 黄志超¹, 李小强²

(1. 华东交通大学 材料科学与工程学院, 江西 南昌 330013)

(2. 华南理工大学 国家金属材料近净成形工程技术研究中心, 广东 广州 510640)

摘 要: 在钎焊温度 1140~1220 °C、钎焊时间 30 min 的工艺参数下, 采用 Ti-9.5Cu-8Ni-8Nb-7Al-2.5Zr-1.8Hf (质量分数, %) 非晶钎料成功实现了 Ti₅₀Al₅₀ (at%) 合金的真空钎焊连接, 并研究了钎焊温度对钎焊接头的显微组织、剪切强度的影响规律。结果表明, 在任何钎焊温度下获得的 Ti₅₀Al₅₀ 钎焊接头均有 3 个界面反应层且每个反应层都含有 α₂-Ti₃Al 和 Ti₂Cu(Ni) 2 个物相。随着钎焊温度的增加, α₂-Ti₃Al 和 Ti₂Cu(Ni) 在钎焊接头中的尺寸与分布发生了明显的变化, 尤其是等温凝固层 II 中的 Ti₂Cu(Ni) 相。1200 °C 下稳定存在的连续 α₂-Ti₃Al 层 I 对母材和钎料原子的相互扩散具有阻隔壁垒作用, 温度一旦超过 1200 °C, α₂-Ti₃Al 相变得不稳定使得连续 α₂-Ti₃Al 层被打破从而失去阻隔壁垒效应。在钎缝中析出且弥散分布的 α₂-Ti₃Al 对焊缝中物相的形成可以起到抑制形核和细化晶粒的作用。随着钎焊温度升高, Ti₅₀Al₅₀ 钎焊接头平均抗剪切强度先增加后减小, 在钎焊温度 1180 °C、钎焊时间 30 min 时钎焊接头的抗剪切强度最大, 达 184 MPa。剪切断面表面呈典型解理断裂特征且 α₂-Ti₃Al 占绝大多数。

关键词: Ti₅₀Al₅₀ (at%) 合金; Ti-Cu-Ni-Nb-Al-Zr-Hf 非晶钎料; 真空钎焊; 显微组织; 剪切强度

作者简介: 李 力, 男, 1979 年生, 博士, 副教授, 华东交通大学材料科学与工程学院, 江西 南昌 330013, 电话: 0791-87046161, E-mail: liliejtu.@163.com